CONF-8802127--3

PROCESSING AND QUANTIFICATION OF X-RAY ENERGY DISPERSIVE SPECTRA IN THE ANALYTICAL ELECTRON MICROSCOPE*

N. J. Zaluzec
Electron Microscopy Center for Materials Research
Materials Science Division
Argonne National Laboratory
Argonne, IL 60439 USA

CONF-8802127--3

DE89 003654

AUGUST 1988

DISCLAIMER

*Work supported by the U.S. Department of Energy, BES-Materials Sciences, under Contract W-31-109-Eng-38.

INVITED KEYNOTE PAPER was presented at the Workshop on "Electron-Beam Induced Spectroscopies at Very High Spatial Resolution", Aussois, France, March 1988.

Processing and Quantification of X-ray Energy Dispersive Spectra in the Analytical Electron Microscope

Nestor J. Zaluzec
Electron Microscopy Center for Materials Research
Argonne National Laboratory
Materials Science Division- 212
9700 S. Cass Ave.
Argonne, Illinois, 60439 USA

Abstract

Spectral processing in x-ray energy dispersive spectroscopy deals with the extraction of characteristic signals from experimental data. In this text, the four basic procedures for this methodology are reviewed and their limitations outlined. Quantification, on the other hand, deals with the interpretation of the information obtained from spectral processing. Here the limitations are for the most part instrumental in nature. The prospects of higher voltage operation does not, in theory, present any new problems and may in fact prove to be more desirable assuming that electron damage effects do not preclude analysis.

Introduction

X-ray Energy Dispersive Spectroscopy (XEDS) in the Analytical Electron Microscope (AEM) has quite literally become a standard tool in the general microstructural characterization laboratory. However, during the last decade virtually no new methodologies in spectral processing have been developed which have had a major impact upon XEDS. This is an indication that data reduction in XEDS has become a mature and reasonably well understood technique. Quantification limitations on the other hand, still persist and in the main can be attributed to instrumental artifacts, specimen preparation and/or variability in XEDS detector manufacture. The prospects for the future for quantification, unlike spectral processing, do not appear to be reaching a plateau. On the contrary, it is more likely that the next generation of instruments, namely: UHV medium voltage instruments with high brightness sources may prove to be the limiting factor in the application of x-ray spectroscopy to the characterization of the local composition of a specimen.

Spectral Processing

Spectral processing, as we shall use the term, deals specifically with the extraction of characteristic x-ray signals from a data set recorded using a solid state energy dispersive detector. The data might be recorded by either a Lithium drifted Silicon (Si(Li)) or high purity Germanium (HP-Ge) spectrometer mounted on the column of a transmission electron microscope. Although the process of x-ray generation results in the emission of characteristic x-ray photon lines from the specimen only a few electron volts in width, their measurement by a solid-state detector broadens that line is into a Gaussian shaped peak, whose width is energy dependent. The effect of broadening is substantial if the amplitude of the natural emission line is given by A, then it will be measured as a Gaussian shaped peak (fig 1) of FWHM = 2.355σ, and amplitude $A^* = A/(\sqrt{2\pi}\,\sigma$ (with$\sigma = \sqrt{K + \varepsilon FE}$, where E is the photon energy in eV, ε the energy needed to create an electron-hole pair ~3.58 for Si, and ~2.94 for Ge, F the Fano factor ~ 0.11-.13 and K the electronic noise of the system). For example, if the amplitude of the emission line at ~ 6 keV was 10^3 counts then the typical solid state detector would measure as a peak amplitude of ~ 60 counts having a FWHM of ~ 150 eV. In addition to this broadening, these detector systems exhibit a series of signal processing artifacts which include low energy tailing due to incomplete charge collection, escape peaks, sum peaks, pulse pileup, and microphonics[1,2]. A general discussion of these issues is beyond the scope of this manuscript.

The ultimate goal of utilizing x-ray spectroscopy in the AEM is generally directed toward quantitative analysis, that is the determination of local atomic concentrations by measurement of characteristic emission from the specimen. The function of spectral processing is to accurately determine the integrated intensity of the x-ray peaks above any background in the experimental spectra, and typically integrals over the peak full-width or full-width at half maximum values (FWHM) are evaluated. For the quantification methods used today, there is no difference which of these value is utilized since both represent a constant fraction of the total x-ray emission, however when considering statistical interpretation the total intensity is preferred [3]. Experimental spectra are composed of two components, the characteristic peaks which are superimposed on a slowly varying continuum of

bremsstrahlung radiation (fig 2). In order to accurately determine the peak areas, this continuum background must be removed.

The simplest methodology in spectral processing ignores the details of spectral shape and concentrates on manual peak integration. Regions of interest are defined in the spectrum and a straightforward summation of the number of counts within the selected window is evaluated yielding the total (peak + background) intensity, $I_T = I + B$ (fig. 3). To correct for the background points either side of the characteristic peak are defined and a simple linear interpolation is used to subtract the continuum contribution (B). A variation of this method is sometimes employed when computerized analysis systems are not available. In this case, narrow windows on either side of the peak of interest are used to to define a background window ($B = B_1 + B_2$) which is then manually subtracted to provide estimated peak integral. There are two disadvantages to this methodology. The first occurs in regions of high background curvature where the linear model does not accurately predict the continuum shape. The interpolation and extrapolation errors will introduce peak integration errors which translate directly into a composition uncertainty. The second deficiency arises from the inability of this procedure to deal with spectral overlaps, which are inherent in the poor resolution of the solid state detectors. Here one may not be able to extract the relative intensities or model the continuum due to the proximity of neighboring x-ray peaks. These can be appreciated in fig 2, which shows an x-ray spectrum taken from a Ti-Ni-Cu-Si alloy. Spectra overlap at the Cu $K\alpha$/Ni $K\beta$ peaks is severe and the non-linear shape of the background is clear.

In order to over come these difficulties, microcomputer-based data acquisition systems have been developed over the last two decades which come equipped with elaborate spectral analysis programs. The data reduction methods employed in these systems can be divided into three basic types. Curve fitting algorithms, which use a combination of non-linear background modeling together with gaussian profile matching to extract intensities. Frequency or digital filtering, which is a method of background suppression and is subsequently used with reference spectra matching to obtain integrals. Lastly deconvolution programs, which employs Fourier analysis techniques to remove background and improve detector resolution.

The curve fitting procedures all require that the experimentally measured spectra be stripped of its continuum or background component in

some fashion. While in the past it was conventional to model and subtract the continuum before proceeding, at the present the continuum is modeled but usually retained and included in the fitting algorithm. Background modeling can vary in its implementation from simple linear segmentation based upon interpolation between user identified background points, through empirical methods employing polynomial expressions, to theoretically predicted background shapes [5-7]. The utility of each of these methods depends upon the intrumental artifacts which are present in the AEM system. Many systems even today are still plagued by the presence of uncollimated radiation produced in the probe forming system causing fluorescence of the specimen and its immediate environs [1,4,8,9]. Since the effects of this uncollimated radiation cannot be modeled it will adversely affect data analysis schemes which employ theoretical models of electron excited bremsstrahlung. As always, it is in the analysts best interest to spend the time to optimize the AEM system to remove/minimize all spectra' artifacts. The procedures for this are well documented in the literature [4]. In light of this, the empirical polynomial expressions might prove to be the most generally applicable to the AEM, even though one would like to think that the theoretical models should work.

Curve fitting, or profile matching as it is sometimes called, proceeds after background correction,by matching the experimental spectra to theoretical peaks or to reference spectra by implementing multiple least-squares (MLS) minimization techniques. The results are then reported as integrals of the theoretical spectra which best match the experimental profiles. If reference spectra are used, then the algorithms return a constant or K-ratio for each analyzed line. This K-ratio value corresponds to the amount of each of the reference lines in the experimental spectrum.

When the MLS analysis is based upon theoretical spectra, the data is generally modeled as a series of nominally Gaussian shaped peak. (Note: we shall not consider further the effects of incomplete charge collection, etc. to the data processing algorithms). This shape function characterized by three parameters shown in figure 1 and is defined by the equation:

$$I(E) = A \exp\left(\frac{-(E-E_C)^2}{2\,\sigma^2(E_C)}\right) \qquad (1)$$

where A is the peak amplitude, E_C the centroid energy and $\sigma(E_C)$ the standard deviation of the peak (FWHM= 2.35 σ). The task a hand is to take the experimental spectra which may consists of several overlapped peaks and find the best solution set of the triplet parameters (A,E,σ) for each peak, which when summed together duplicates the experimental data profile as illustrated in figure 4. At this point we can subdivided the MLS curve fitting procedures into two branches namely the linear and non-linear algorithms.

In the linear methods, one assumes that the data acquisition is calibrated and thus the values of the peak centroids (E_C) and the peak widths (σ) are are accurately known. If this is the case then one can write a simple matrix equation which describes the experimental profile. Letting y_i represent the data at the point i, then we can write for any point in the spectrum the equation:

$$y_i = \sum_{i=1}^{N} A_k G_{ik}, \qquad \text{with } G_{ik} = \exp\left(\frac{-(E_i-E_k)^2}{2\sigma^2(E_k)}\right) \qquad (2)$$

Since the values of E_k, and $\sigma(E_k)$ are known for each of the N peaks in the spectrum, equation 2 reduces to a simple algebraic (matrix) equation of N variables and N unknowns, which can be solved directly for the peak amplitudes A_k. Knowing A_k, one can then directly compute the peak integrals. This method is fast, simple and reliable, however it does require that the XEDS microanalysis system be precisely calibrated for centroid energy positions as well as the variation of σ with energy. Today, most commerical XEDS systems have semiautomatic calibration programs and therefore this does not present any major difficulties. Alternatively each spectra can be individually calibrated prior to the analysis which, in effect, yields the same result. We have also implicitly assumed that the analyst has determined precisely which x-ray peaks to fit to the data set. Should a line be omitted from the fit then subsequent errors will be encountered in the resulting reported integrals.

The non-linear modeling approaches to this problem are less restrictive in their requirements. These methodologies do not presume exact calibrations, but instead rely on the computer to search a three dimensional parameter space (for each peak) to find the best fit to the data by iterating A, E_k and $\sigma(E_k)$ to minimize the quantity X^2, which is defined as:

$$X^2 = \sum_{k=1}^{M} \left(\sum_{i=1}^{N} \frac{(y_i - Y_k)^2}{y_i^2} \right) \quad \text{with } Y_k = A_k \exp\left(\frac{-(E_i - E_k)^2}{2\sigma^2(E_k)} \right) \quad (3)$$

here Y_k is the theoretically modeled k^{th} peak intensity at energy E_i, and y_i is the experimental data all other parameters having been defined previously. There are two general search procedures employed to explore parameter space to minimize X^2 : they are the pattern and gradient search methods.

In the pattern search methods one can either sequentially iterate through parameter space changing systematically each of the values of the triplet (A,E,σ) until a local minimum is found, or use a geometric approach where all three parameters are varied simultaneously in a prescribed manner. The former method is essentially mechanical in nature. Here, one computes X^2 over a grid in the 3M parameter space (M is the number of peaks being fitted) and inspects this matrix for a local minimum. Usually systematic iterations of each parameter are used in the minimization algorithms, which are then repeatedly incremented for each of the terms (A,E,σ) in each peak until a local minimum is found. In contrast, the geometric or simplex method is more elegant in that it reduces the number of iterations needed to find a local minimum by a simultaneously varying all 3 parameters for each peak at each iteration [8,9]. In a simplex analysis, the possible solution vectors of a fit can be visualized as a forming polygon in 3M space and containing M+1 vertices, each vertex representing a triplet vector (A,E,σ). The optimization procedure begins by computing X^2 for each of the initial M+1 guesses, one of which will represent least desirable value of X^2 in the first iteration. Having calculated X^2, one next constructs a new solution vector for the next X^2 iteration by reflecting the parameters of the least desirable vector (A,E,σ) -->(A^*,E^*,σ^*) perpendicular to the centroid of its neighbors (i.e moving away from the greatest X^2 value as schematically illustrated in fig. 5). The new set of M+1 X^2 values are then reinspected and the next least desirable vector is identified. A reflection operation is implemented and the process continues until convergence is obtained. The advantage in this approach resides in the fact that each computation changes all three parameters of the fit at each

iteration, thus the overall speed relative to the brute force method is enchanced.

The common problems associated with both of these search procedures is the errant identification of local minima as solutions, rather than reaching the true global minimum. In order to minimize this error one must necessarily start with estimates of the parameter space triplet (A,E,σ) which are not grossly in error. Of these three parameters the peak centroid energy (E) is most important, while the amplitude (A) is least important. However, there is always the possibility for the system to find mathematically correct yet non-physical solutions in extreme cases of spectral overlap [11], operator insight here is always a key factor.

The gradient search methods are the next level in refinement in MLS analysis [10]. Rather than sequencing through an array of values as in the pattern searchs, this method tries to predict in which direction in 3M space the true solution set exists. Here, the value of $\frac{d^2X^2}{d^2p}$ is numerically evaluated at each of several directions in parameter space and the direction of steepest negative gradient is determined. This gradient will always point in the direction which causes the greatest change in X^2, thereby, in theory, increasing the speed which the solution vector (A,E,σ) is found since fewer values should need to be interrogated. In practice, the initial X^2 gradient is computed by incremental changes in the (A,E,σ) vectors and an iteration direction defined from this initial estimate. The parameters of (A,E,σ) are incremented along that vector until a local minimum is attained. At that point a new gradient vector is determined and the process repeated until suitable convergence is reached. The disadvantage to this procedure is that the gradient only indicates a direction and not a magnitude and the method tends to converge slowly in situations where the X^2 surface is relatively flat.

An alternative method has also been developed which bridges the gap between the linear and fully non-linear procedures. Termed multiple least squares with derivitive reference, this method attempts to linearize to the more general fitting problem when calibration errors exist and reference spectra are employed [12-14]. The problems implicit in using reference spectra instead of theoretical profiles, are relate directly to the calibrations of the detector system. In general unless the reference spectra and the unknown have been recorded under identical conditions the calibration errors can

prohibit exact profile matching. In the derivitive reference approach, Kitazawa et al.[13] have shown that if the spectral calibration errors are small, then the perturbed Gaussian profile can be expanded in a Taylor series and represented as a simple linear combination of the reference spectrum and its first and second derivatives. Using this methodology fitting errors of less than 1% can be routinely obtained, when spectral shifts are less than about 20 eV. The advantage of this approach over that of theoretical modeling lies in the fact that the reference spectra necessarily include all detector related distortions to the peak profiles. Thus the additional step of modeling, for example: the low energy tailing, in the EDS detector is eliminated. The disadvantage is that one must prerecord standard spectra for all elements which are to be analyzed.

A variation to the curve fitting approach presented above is one which employs digital (frequency) filtering for background removal. After filtering the background component from the spectrum, characteristic peaks are fitted using a conventional MLS analysis as already discussed. The concept of digital filtering can be best visualized by considering it to be a numerical differentiation of the data combined with a smoothing of the spectrum over a limited spectral window. Digital filtering is implemented by convoluting a simple linear (top-hat shaped) weighting function (fig.6) with the experimental data. If the XEDS intensity is given by f(x) then we can define a tophat filter function (G(x)) of the data set x_j by the equation :

$$G(x_i) = [\ F(x_{+1})\ -\ 2*(\frac{W_-}{W_+})*\ F(x_0)\ +F(x_{-1})] \qquad (4)$$

where $F(x_j) = \Sigma\ f(x_j)$ with the summation is evaluated over the width of each of the three respective windows (x_0 = central, x_{-1} = left, x_+=right) as defined in figure 5. The scaling factor $2W_-/W_+$ results if the respective widths of the positive and negative windows are different and its effect is to force the digital filter to become one of zero-area, that is the net area of the central positive window is equalivent to the sum of the areas of the two negative windows. One can show by simple substitution that if the function f(x) is linear i.e. of the form f(x) = m x + b, then the quantity G(x) is identically zero at all times. Thus the application of a digital filter as given by equation 4 to any linear function yields a new (transformed) function G(x) having zero

slope and intercept, and by extension its application to any combination of linear background and non-linear spectral feature will result in the complete removal of the linear component (fig 6). Figure 7 shows an example of this type of filter applied to the data of figure 2, where for the sake of visibility we have expanded the vertical scale to show the background both before and after the filtering. For XEDS, Statham has shown that the optimum width of the filter window to be W_+= FWHM and W_-= 0.5*FWHM [15]. The advantage of this method for background correction rests in the fact that it is operator independent and thus does not rely upon the human judgement, however as can be seen from figure 7 it introduces severe spectral distortion. For application to MLS analysis the filter is applied to both the reference and unknown spectra and relative intensities extracted as discussed previously.

The last method, which has receive little application in the AEM environment, is that associated with Fourier analysis techniques [16-19]. The objective of this technique is to enchance the resolution of the solid state detector. Here, one attempts to find a set of x-ray lines and relative intensities which when convoluted with the response (broadening) function of the EDS system duplicates the experimental profile. As in the case of the curve fitting procedures, a background model must be employed to remove continuum, which is then followed by a Fourier Transform of the remaining spectral profile. Next deconvolution using a modeled detector response function and then back transformation to obtain the resolution enhanced data. In ideal cases, where the experimental data set is not noise limited, the procedures can produce impressive results[16]. However, in more practical situations, statistical noise in the experimental data prohibits the application of this method to AEM based analyses. Resolution enchancement of ~65% FWHM can expected in typical cases where noise is not the limiting factor.

Quantitative Analysis

Given that we have now extracted the relevant peak intensities one asks the question: what factors govern the accuracy of the quantitative results? If we use the conventional ratio technique [20] for AEM thin film analysis then the relationship between measured x-ray intensity (I) and the local composition (C) of for any two elements (A,B) in the specimen is the familiar formula:

$$\frac{I_A}{I_B} = \frac{\kappa_A \varepsilon_A C_A}{\kappa_B \varepsilon_B C_B} = k_{AB}^{-1} \cdot \frac{C_A}{C_B} \qquad (6)$$

$$\text{with } \kappa_A = \frac{\sigma_A \omega_A \Gamma_A}{W_A} \qquad (7)$$

where σ = ionization cross-section, ω= fluorescence yield, Γ= radiative partition function, W=Atomic Weight, N_O, ρ = Avagodro's number & density, and ε = detector efficiency for each element.

The accuracy of quantification using this ratio technique is from equation 6 directly tied to the accuracy in which one can determine the value of $\frac{\kappa_A \varepsilon_A}{\kappa_B \varepsilon_B} = k_{AB}^{-1}$. Experimental determinations of k_{AB} have been done by a variety of independent investigators, and they have been generally been reproducible over a limited range of Z, but not universally so. Although equation (6) is a simple and elegant relationship it is important to realize that the factor k_{AB}^{-1} should not be considered a universal constant. The reason for this can be appreciated by noting that k_{AB}^{-1} is the product of two terms. The first κ_A/κ_B, the ratio of the x-ray generation constants, is a real physical constant of a solid and is independent of the AEM used to generate the data (at constant accelerating voltage). The second $\varepsilon_A/\varepsilon_B$, the detector efficiency ratio is an experimental factor, which can vary from one system to another due to the variablity in the manufacture of the solid state detectors. Since ε can vary from one AEM/EDS system to another (or even with time in a single system due to contamination), it should not be surprizing that experimental k_{AB}^{-1} factor show deviations, even when all appropriate specimen related corrections are applied.

The effect of detector variation on k-factor was demonstrated by two independent round robin studies in 1984. These studies attempted to measure the stability of quantitative analysis on reference specimens consisting of a Stainless Steel alloy and a NiO compound sent to a variety of laboratories in the U.S. To appreciate the significance of this work let us first refer to figure 8, which plots the theoretical detection efficiency for a windowless solid state detector systems. From this figure one can see that in the photon energy range of ~ 5-20 keV the efficiency of a Si(Li) detector is essentially constant. This being the case, then one would expect experimentally measured compositions (or equivalently k-factors for standards) for x-ray lines in this range to essentially be independent of AEM/Si(Li) detector system. This has

been experimentally confirmed by the Vitek et al. study [21] which considered the Fe-Ni-Cr system. In contrast, for x-ray photons of widely seperated energy, particuliarly when one line is < 3 keV, one would expect detector variablity to be most visible. In this regime, the detectors are particuliarly sensitive to their manufacture, being influenced by the various absorbing windows (Be, Au, Si Dead Layer,....) which are present. The Thomas et al study on NiO confirms this expectation [22]. These results clearly indicate that the detector itself can greatly affect the accuracy of the analysis reported, and significantly point to the fact that the nominal parameters quoted by the respective manufacturers are just that and should not be taken with any level of confidence.

If this is the case then, we are in a serious dilemma. To obtain reliable analysis these arguments indicate that we must each generate a complete set of standard reference specimens to calibrate our respective detectors for the range of elements of interest. This, of course, is extremely tedious, however it may be the only method of accurate quantification. As an alternative, one could use a smaller subset of composition standards and appropriate theoretical/experimental models to calculate the parameters of $\kappa_A = \frac{\sigma_A \omega_A \Gamma_A}{W_A}$ and then back-calculate the best fit or effective detector parameters[1]. This would provide a self consistent set of relationships which could be used in lieu of attempting to obtain references specimens for every possible elemental configuration and would appear to be a reasonable compromise when it is not possible to obtain appropriate standards.

Given the apparent strong effects of Si(Li) detector efficiency, it is interesting to consider what might be encountered with the new HP Ge detectors which have been discussed recently [23]. Figure 8 shows that an extremely strong Ge L absorption effect (due to the Ge dead layer) will have a pronounced effect on the overall efficiency at the low energy end of the spectrum. This will undoubtable be observed in any $k_{A\,B}$ factor determinations, but to a greater degree than the Si(Li) case just discussed. With the minor exception of a small drop in efficiency at the Ge K edge (~ 10 keV), the high energy response of these detectors appears excellent.

Lastly let us finish by considering the prospects for quantification in lieu of the impending availability of medium voltage AEM's. Referring to equation 7, the only term in the quantitative analysis which is voltage

dependent is σ, the ionization cross-section. For the medium voltage regime it is clearly important to employ relativistic formulations for σ as the discrepancy between the non-relativistic and relativistic models increases with accelerating voltage, as shown in figure 8. Ideally, one would like to utilize some of the more accurate theoretical calculations of cross-section such as those of Scofield [24] or Rez [25], unfortunately the available data does not cover the requisite atomic number/ accelerating voltage regime in AEM. As an alternative, parameterizations have been developed which essentially cover the entire AEM operating environment and agree quite well with these more specific studies for both the K and the L shell transitions [26]. Using this set of parameterized cross-sections one can calculate the expected variation in the K-shell ionization cross-section ratio with accelerating voltage, which is shown in figure 10. Here we plot the Al/Ar, Al/Ni, and Al/Ag cross-section ratio from 50 to 1000 keV. We note that as the atomic number difference in the elements increases, so does the variation in σ_A/σ_B with voltage. Further for a given pair of elements, as the voltage increases the variation in σ_A/σ_B and thus k_{AB}^{-1}, will decrease. This implies that the quantitative analysis as a function of voltage should be less sensitive to the AEM beam energy as we increase the incident beam energy. Unfortunately, increasing the operating voltage of the AEM may result in electron damage effects which can modify or destroy the specimen during the analysis [27].

Concluding Remarks

Spectral processing in XEDS for the AEM environment has reached a relatively stable point. The procedures and computer processing power is now available to all analysts and should present no major difficulites to data reduction, provided the operator insures the data acquisition system is reasonably well calibrated. Quantitative analysis, on the other hand, still can suffer from instrumental limitations which for the most part can be attributed to detector efficiency variability or specimen preparation artifacts. The advent of higher voltage AEM should not introduce any difficulities to quantification.

References

1.) N. J. Zaluzec EMSA Bulletin 14, #1, 67 (1984), 14,#2, 61 (1984), 15, #1, 67 (1985)

2.) D.A. Gedcke, X-ray Spectrometry, 1, (1972), 129

3.) P. Trebbia, These proceeedings

4.) J. Bentley et. al. SEM/1979/Vol II, SEM Inc. AMF O'Hare, 581-594

5.) P.J. Statham, X-ray Spectrometry 5, (1976), 16-28

6.) Nicholson etal - AEM 1984, San Franc. Press Ed. D.B. Williams, D.C. Joy, (1984), 258

7.) C.E. Fiori, C.R. Swyt, J.R. Ellis, Microbeam Analysis-1982, San Fanc. Press, Ed. K.F. Heinrich (1982),57

8.) J. Bentley etal Materials Research Society Symposium Proc. 41, 363-368 (1985),

9.) J.P. Chevalier, These proceedings

8.) S.N. Deming, S.L. Morgan, Anal. Chem. 45 , (3) , (1973) 379A

9.) C.E. Fiori, R.L. Myklebust, in Computers in Activation Analysis and Gamma-ray Spectroscopy, Technical Information Cen./ U.S. Dept of Energy, (1979) 139-149

10.) P.R. Bevington, Data Reduction and Error Analysis for the Physical Sciences, McGraw Hill (1969), Chapter 6-12

11.) P.J. Statham, X-ray Spectrometry 7, (3), 132, (1978)

12.) F.H. Schamber, Microbeam Analysis-1973, (1973), 85

13.) MLS Kitazawa, Shuman, Somlyo, Utramicroscopy 11, (1983), 251

14.) D.J. McMillan, G.D. Baughman, F.H. Schamber, Microbeam Analysis-1985, San Fran. Press. Ed. J.T. Amstrong (1985) 137-140

15.) P.J. Statham, Analytical Chemistry, 49, #14, (1977), 2149-2154

16.) H.J. Hay, Nuclear Instrum & Methods in Physics Res. B10/11 (1985), 624-628

17.) P.J. Statham 8th Int Conf. on X-ray Optics and Microanalysis.,Pendell Pub.Co. Ed. D.R. Beaman, R.E.Ogilvie,D.B. Wittry, (1980), 136-140

18.) P.A. Jansson, R.H. Hunt, E.K. Plyer, J. Opt.Soc. Am. 60,(5), 596-599 (1970)

19.) B. Roy Frieden, J. Opt.Soc. Am. 62,(4), 511-518, (1972)

20.) N.J.Zaluzec , in Analytical Electron Microscopy, Plenum Press, Ed. D.C. Joy, J.I. Goldstein, J.J. Hren, (1979) Chapter4, 121-168

21.) J.M. Vitek, Analytical Electron Microscopy-1984, San Francisco Press, Ed. D.B. Williams and D.C. Joy (1984), 374-376

22.) L.E. Thomas et al. Ibid, 333-336

23.) These proceedings

24.) J.H. Scofield, Atomic and Nuclear Data Tables 14, 121, (1974)

25.) P.Rez, X-ray Spectrometry, 13, 55, 1984

26.) N.J. Zaluzec, in Analytical Electron Microscopy-1984, op cit. 279

27.) C.R. Bradley and N.J. Zaluzec, these proceedings

28.) This work was supported in part by U.S. DoE , contract BES-MS W-31-109-Eng-38 and the Aussois Workshop through grants from the French CNRS and U.S. NSF.

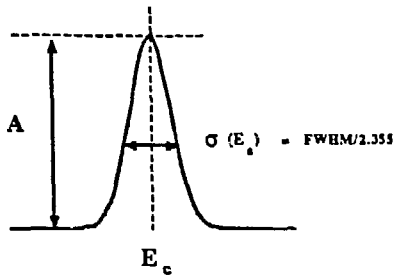

Figure 1. Definition of the parameters of a Gaussian Distribution

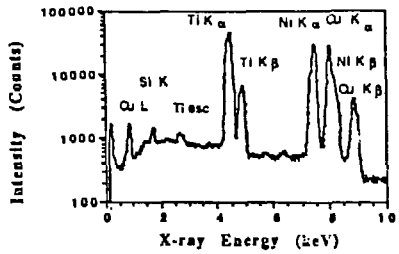

Figure 2.) Typical X-ray spectrum generated in an AEM, showing characteristic peaks and continuum background

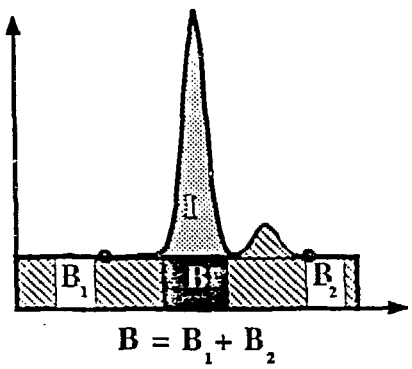

Figure 3. Definitions of peak intensity (I) and background (B) regions used in simple quantitative analysis

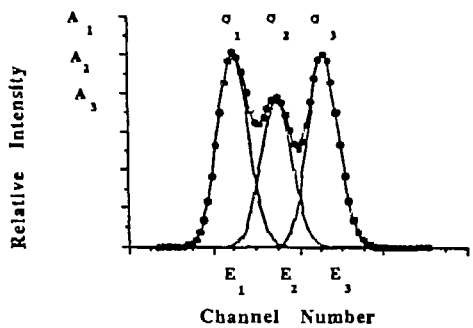

Figure 4. Overlap of Gaussian peaks resolved into their individual component distributions

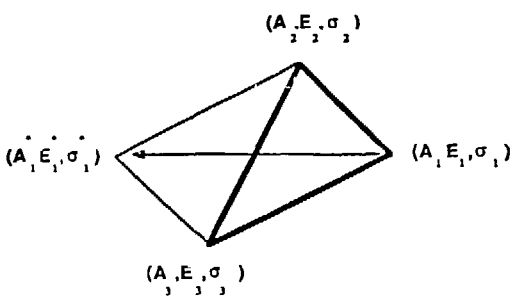

Figure 5. A two dimensional representation of the sim geometric construction and its reflection operation to ...ain a new iteration vector

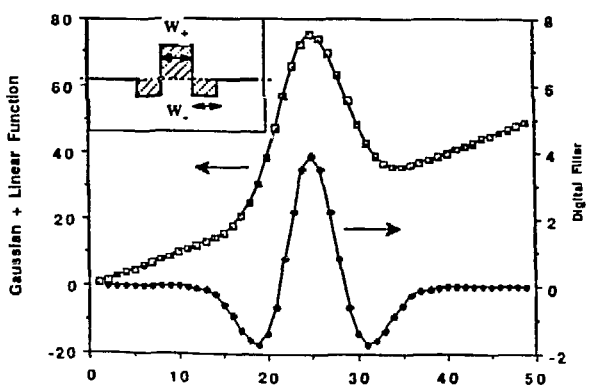

Figure 6.) Schematic illustration of a top-hat filter function used for background removal in XEDS data analysis and an example of its effect upon a Gaussian peak superimposed upon a linear backgro